

## Chemistry in disks and planets

# Zooming in on the Chemistry of Protoplanetary Disks with ALMA

L. Ilsedore Cleeves

Harvard-Smithsonian Center for Astrophysics  
60 Garden St MS-51  
Cambridge, MA 02138, USA  
email: [ilse.cleeves@cfa.harvard.edu](mailto:ilse.cleeves@cfa.harvard.edu)

**Abstract.** During the first few  $\sim$ Myr of a young stars life, it is encircled by a disk made up of molecular gas, dust, and ice – the building blocks for future planetary systems. How/when these disks form planets and what sets the planets initial compositions remain key outstanding questions in disk science. In recent years, major leaps in sensitivity and spatial resolution afforded by the Atacama Large Millimeter/Submillimeter Array (ALMA) have revolutionized our understanding of protoplanetary disks chemical composition and physical properties, revealing in some cases complex radial, vertical, and azimuthal structure in the dust and gas. In this contribution, I review recent observational results and new theoretical puzzles, and how these fit into a newly emerging picture of the disk environment.

**Keywords.** planetary systems: protoplanetary disks, astrochemistry

---

## 1. Introduction

Protoplanetary disks are complex systems of gas, dust, and ice, that over the course of millions of years assemble new planetary systems. Understanding their compositions can thus inform our understanding of the initial composition of “typical” planetesimals. In the six years between the previous astrochemistry symposium in 2011, IAUS 280: “The Molecular Universe” in Toledo, Spain, and the present symposium, the 2017 IAUS 332: “Through the Cosmos from Galaxies to Planets” in Puerto Varas, Chile, we have gone from the pre-ALMA to the post-ALMA era. ALMA has brought order(s) of magnitude improvement in spatial resolution and in sensitivity. And though ALMA has not (yet) substantially increased the observed molecular inventory in disks (as of the meeting, only adding  $\sim$  25% to our known list of radio-detected molecules); instead, ALMA’s sensitivity has enabled us i) to make high spatial and spectral resolution maps with unprecedented signal to noise and ii) to measure the rarer isotopologues that peer deeper into gas where the main isotopologues are thick.

Of the most striking results out of ALMA is the the prevalence of ring-like structure. Some of the most famous rings are those seen in the continuum as either fine-ringed structure (e.g., ALMA Partnership *et al.* 2015; Andrews *et al.* 2016) or large inner gaps/asymmetries (e.g., van der Marel *et al.* 2013). However, the chemistry has offered perhaps even more complex puzzles regarding the varied distribution of emission between molecules for the same disk, and between different disks for the same molecule.

Understanding the nature of this highly structured molecular emission is a highly active area of research. Generally interpretations fall into three broad camps, which include i) changes in the “true” abundances of molecules with distance from the star and/or height, ii) changes in the excitation conditions (temperatures/densities), and iii) deficits in bulk H<sub>2</sub> gas within cleared out “rings” (e.g., Isella *et al.* 2016; Teague *et al.* 2017). Moreover many of these interpretations can operate even within the same disk. Thus observing

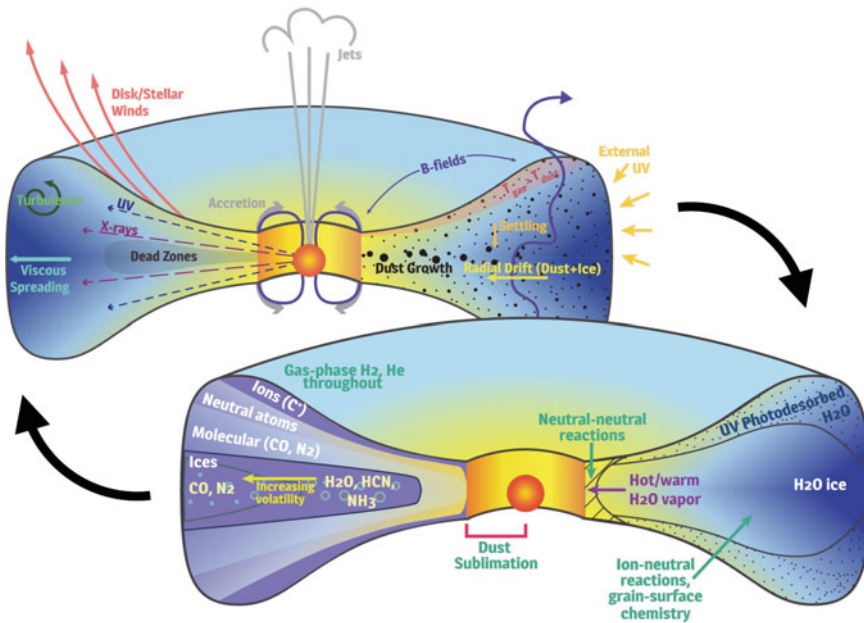


**Figure 1.** Cartoon illustrating the complex, co-existing chemical and physical processes that are thought to occur in protoplanetary disks. From Cleeves (2015, PhD thesis).

many molecules at relatively high ( $\gtrsim 0.3''$ ) resolution is necessary to disentangle, for example, scenario i) vs. iii).

To begin interpreting these ring-like structures, we can utilize our knowledge of the sensitive links between the local chemical composition and the physical conditions of the gas and dust (e.g., Bergin *et al.* 2007). At the most basic level, the temperature of the gas and dust determine where molecules predominantly reside in the gas or ice phase. In the midplane, the radial position at which this transition occurs is called the snow line (see Sections 2.1 and 2.2). The gas density of the disk regulates the rate at which reactions can occur, but also provides a source of shielding that can shadow the deeper layers of the disk from radiation. The dust itself provides a substrate to facilitate the formation of water and complex organics in the ice-phase chemistry; however, it too grows and evolves via coagulation and fragmentation over the lifetime of the disk (Testi *et al.* 2014), impacting the chemistry in recently discovered ways (see Sections 2.2 and 3). Simultaneously, much of the grain-surface chemistry and broader gas-phase chemistry occurring in cold gas is sensitive to the ionization state of the disk, which can come from many sources (e.g., Glassgold *et al.* 1997; Cleeves *et al.* 2013, 2014), and thus understanding the interaction of the disk gas with the varied ionization sources is critical for understanding the active chemical state of the gas and its history (see Section 4).

The present contribution was designed to give an overview and an update of the new results coming out of ALMA since the last astrochemistry IAU symposium. It is not designed to be a detailed review, but rather an attempt to link together various clues that have been coming out over the last six years into just one possible broader narrative. This narrative will undoubtedly change, and has only continued to evolve over the short months between the IAUS 332 meeting in March and these proceedings. Here I attempt to focus on what my contribution covered at time of meeting, but have incorporated new information where necessary.

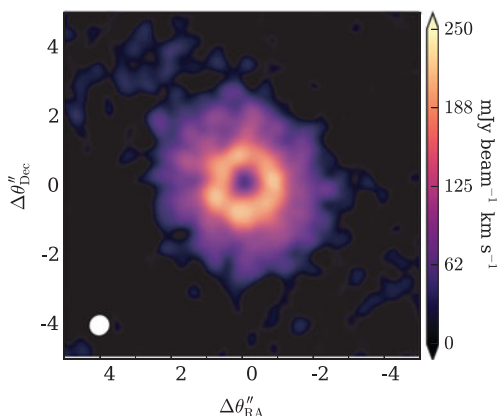


**Figure 2.** Observed distribution of  $\text{N}_2\text{H}^+$   $J = 4 - 3$  in TW Hya. Data from Qi *et al.* (2013).

## 2. A Prevalence of Molecular Patterns

### 2.1. $\text{N}_2\text{H}^+$ and its relationship with CO

Perhaps one of the most notable chemical rings is that of  $\text{N}_2\text{H}^+$  seen in the  $J = 4 - 3$  rotational transition in the TW Hya disk reported in Qi *et al.* (2013). The  $\text{N}_2\text{H}^+$  shows a clear ring-like distribution (see Figure 2) with an inner radius of  $\sim 30$  AU. The chemistry of  $\text{N}_2\text{H}^+$  is such that it is rapidly destroyed in the presence of CO. As a consequence,  $\text{N}_2\text{H}^+$  has been historically used as a marker of CO freeze-out in the dense interstellar medium (Charnley 1997; Bergin *et al.* 2002). Thus the Qi *et al.* (2013) paper interpreted the ring of  $\text{N}_2\text{H}^+$  as a marker of the TW Hya disk's CO snow line, which was also in reasonable agreement with model temperature estimates of the disk at these radii (Qi *et al.* 2013, 2015).

More recently, measurements with ALMA of trace species in Schwarz *et al.* (2016) found a steep drop off of CO intensity at  $\sim 17 - 23$  AU, interior to the  $\text{N}_2\text{H}^+$  ring. These results were more recently supported by  $^{13}\text{C}^{18}\text{O}$  observations reported in Zhang *et al.* (2017), which place the break at a radius of  $20.5 \pm 1.3$  AU. Both papers attribute the steep drop off CO isotopologue emission at this location also to the CO snow line. This spatial discrepancy between the  $\text{N}_2\text{H}^+$  transition and the CO transition is in part due to the inescapable nature of the disk temperature gradients, which are not purely radial. Instead, the vertical increase in temperature with height in the disk (see Figure 3) causes the region of CO freeze-out to occupy a wedge, with  $\text{N}_2\text{H}^+$  in the simplest case bounding its borders until  $\text{N}_2$  freeze-out commences. More detailed modeling of the chemistry (e.g., Aikawa *et al.* 2015; van't Hoff *et al.* 2017) shows that the distribution of  $\text{N}_2\text{H}^+$  is complicated by additional factors, including the desorption rates of CO vs.  $\text{N}_2$ , CO abundance, and disk ionization.

The face-on nature of the disk of the TW Hya complicates the analysis further. Future work on different, more inclined disks, coupled with models, or additional constraints on the radial temperature profile and gas surface density will hopefully shed additional light on the nature of the observed radial transitions and their relationship with CO freeze-out.

### 2.2. Double ring CO emission

New sensitive observations of CO isotopologues have also revealed non-monotonic brightness distributions with distance from the star. More specifically, a secondary ring of CO isotopologue has now been seen in multiple disks (e.g., Huang *et al.* 2016; Nomura *et al.*

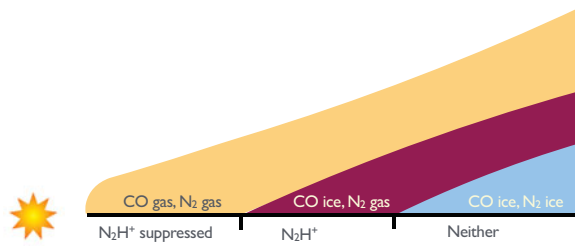


**Figure 3.** Schematic of the “classical” picture of the relationship between  $\text{N}_2\text{H}^+$  and the CO snow line.  $\text{N}_2$  is expected to stay in the gas down to lower temperatures than CO, leading to a layer between the region of CO freeze out and  $\text{N}_2$  freeze out where  $\text{N}_2\text{H}^+$  is expected to occupy. Additional factors beyond these that impact the  $\text{N}_2\text{H}^+$  distribution are described in Aikawa *et al.* (2015) and van’t Hoff *et al.* (2017).

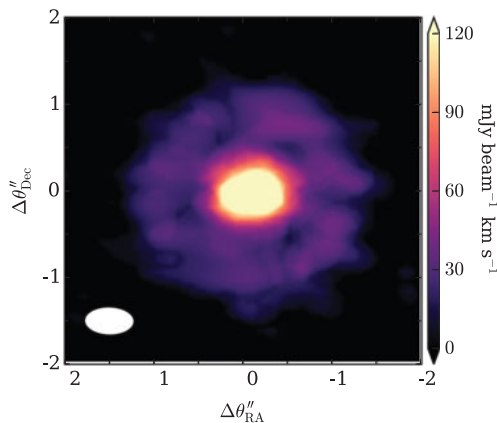


**Figure 4.** Observed distribution of  $\text{C}^{18}\text{O } J = 3 - 2$  in TW Hya, color stretched to highlight the outer ring. Data from Schwarz *et al.* (2016).

2016; Schwarz *et al.* 2016), see Figure 4 for the case of TW Hya from Schwarz *et al.* (2016). The  $\text{C}^{18}\text{O } J = 3 - 2$  emission is centrally peaked, steeply drops off beyond  $\sim 20$  AU, but then rises again at around  $\sim 50 - 60$  AU. This brightening of CO corresponds to the edge of the millimeter emission, which sharply drops off at this point (i.e., the edge is not a “sensitivity” edge but a true deficit of grains, see, e.g., Andrews *et al.* 2012; Hogerheijde *et al.* 2016). Essentially the millimeter emission traces the location of “large” grains (those that have undergone growth). For comparison, the small grains as traced by scattered light extend out to  $\sim 200$  AU (Trilling *et al.* 2001), which is similar to the radius of the gas as traced by  $^{12}\text{CO}$  (Andrews *et al.* 2012).

The re-emergence of CO at these distant radii provides insight into the conditions in the gas locally, namely either there is a temperature transition enabling thermal desorption (essentially a secondary CO snow line) or an opacity transition that allows external (or scattered internal) UV photons to directly photodesorb CO ices.

Cleeves (2016) modeled the disk temperature and UV opacity structure for models that include a truncated distribution of large grains with a continuous distribution of entrained small grains following the gas (see Figure 5). It was found that when millimeter grains are compact, the dust outside of this region can be directly heated by the reprocessed radiation originating from the upper warm layers of the disk. This same reduction in dust opacity also permits UV radiation to reach the outer disk midplane. Which of these two

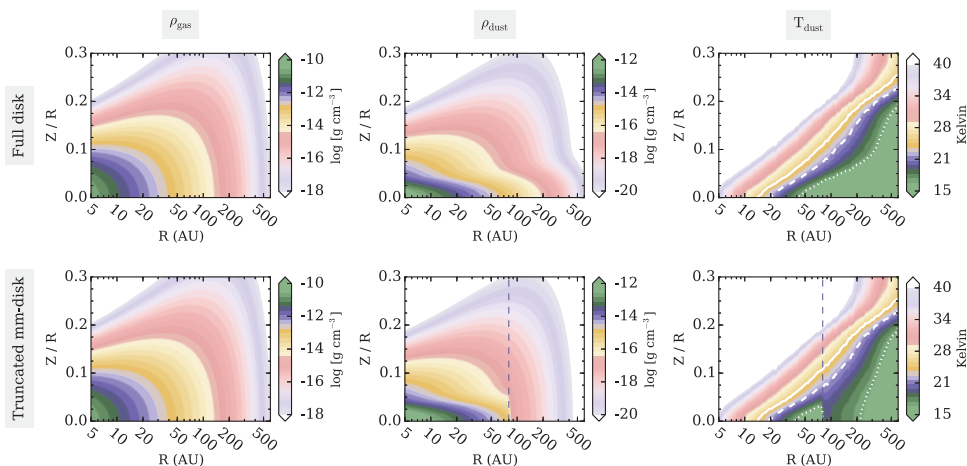


**Figure 5.** Gas density (left), dust density (center) and temperature (right) for models without and with a sharp radial transition in the millimeter dust disk (top and bottom respectively). Reproduced with permission from Cleeves (2016).

processes dominate depends on the size of the millimeter grain disk, e.g., more compact disks tend to favor efficient thermal desorption, while extended disks do not become sufficiently warm and non-thermal mechanisms are expected to dominate.

### 2.3. Deuterated species

In the pre-ALMA era, observational studies of isotope fractionation were only possible on disk-averaged scales, and often using optically thick (bright) species. It is now feasible to image disks on scales corresponding to fractions of an arcsecond (or  $< 50$  AU for disks at the distance of Taurus). ALMA is beginning to map nitrogen isotopic fractionation (Guzmán *et al.* 2015, 2017; Hily-Blant *et al.* 2017) and deuterium fractionation (Huang *et al.* 2017; Salinas *et al.* 2017).

Rings are again commonly seen, and perhaps even more striking is that often the distribution of the less abundant species does not follow that of the more abundant species. As one example, Figure 6 shows velocity integrated emission from  $\text{H}^{13}\text{CO}^+$  and  $\text{DCO}^+$  toward the IM Lup protoplanetary disk (observations from Öberg *et al.* 2015a). The  $\text{H}^{13}\text{CO}^+$  shows a single broad ring, while the  $\text{DCO}^+$  exhibits two narrow rings, almost in diametric opposition to the  $\text{H}^{13}\text{CO}^+$ . In the pre-ALMA era, disk integrated fluxes were often used for isotope ratios, but as can be seen here, how those values translate to real isotopic ratios is not always straightforward.

Generally, deuterium fractionation is expected to be a temperature driven process; lower temperatures tend to favor reactions that incorporate the heavy species over the light ones (e.g., review by Millar 2003). If one visually traces out D/H with distance from the star from Figure 6, it is clear that the profile transitions from a high D/H, to a low D/H in between the  $\text{DCO}^+$  ring, finally returning back to a high value. This could be a non-monotonic radial temperature effect, or instead it could point to multiple fractionation pathways becoming dominant under different conditions (see Huang *et al.* 2017).

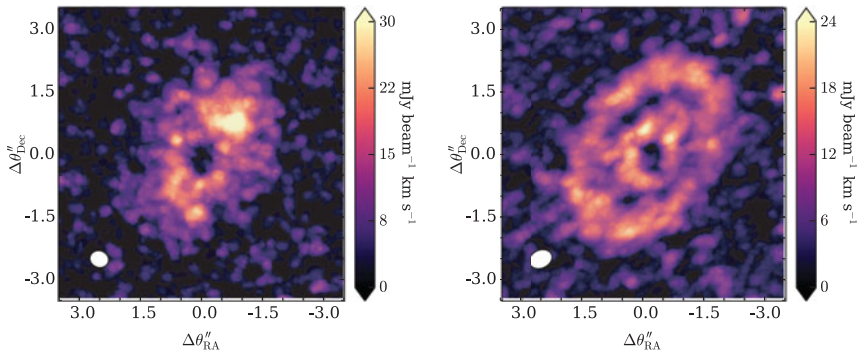


**Figure 6.**  $\text{H}^{13}\text{CO}^+$  (left) and  $\text{DCO}^+$  (right) as observed toward the IM Lup protoplanetary disk. Data from Öberg *et al.* (2015a).

### 3. Volatile Depletion

#### 3.1. Missing oxygen and carbon?

The *Herschel* Space Observatory gave early indications that the volatile reservoir of oxygen in disks may be reduced relative to interstellar gas. More specifically water was found to be under abundant in disks by one to two orders of magnitude (Bergin *et al.* 2010; Hogerheijde *et al.* 2011; Du *et al.* 2017) though with some uncertainty in the specific values due to uncertainty in the chemistry and radiative transfer (Kamp *et al.* 2013). Gas mass measurements from atomic oxygen yielded masses far lower than that expected from the dust for a gas to dust mass ratio of  $\sim 100$  (Thi *et al.* 2010). This pointed to two possible scenarios, a true gas depletion ( $\text{H}_2$ ) or a depletion of oxygen in the observable layers. Part of the solution came from *Herschel* observations of HD, which pointed to a  $\text{H}_2$  gas-rich disks more consistent with measurements from the dust (Bergin *et al.* 2013). It was later found with ALMA that CO was likewise depleted (Schwarz *et al.* 2016), supporting earlier measurements from disk averaged SMA observations (Favre *et al.* 2013; Cleeves *et al.* 2015). Furthermore, Schwarz *et al.* (2016) found that the CO abundance remained low even within a 20 AU radius of the star, the region where thermal desorption should return CO to the gas if it is present. Observations of atomic carbon with APEX also supported that the carbon itself was missing, rather than CO being preferentially dissociated (Kama *et al.* 2016).

McClure *et al.* (2016) reported *Herschel* HD measurements for six more disks, enabling additional volatile abundance determinations. They compared CO depletion factors for those disks whose trace CO isotopologues have been measured, and found that the younger disk, DM Tau, had relatively mild CO depletion, up to a factor of five relative to interstellar. Comparing these values, the depletion in DM Tau's CO is far more mild than that in the older disk TW Hya; however, both disks have similarly high degrees of water depletion (Bergin *et al.* 2010; Hogerheijde *et al.* 2011). This may hint at the timescales for sequestration of oxygen versus carbon, but the sample size is still too small to make definitive statements.

#### 3.2. Hydrocarbons

One surprising discovery regarding the disk molecular inventory was the overall brightness of hydrocarbons, specifically  $\text{C}_2\text{H}$  and  $c\text{-C}_3\text{H}_2$ .  $\text{C}_2\text{H}$  was first detected and imaged with the SMA in TW Hya, and was found to occupy a bright single ring of emission (Kastner *et al.* 2015). ALMA imaged and confirmed the ring-like geometry of  $\text{C}_2\text{H}$  in TW Hya, and found the ring nests outside of the millimeter thermal dust edge (Bergin *et al.* 2016).

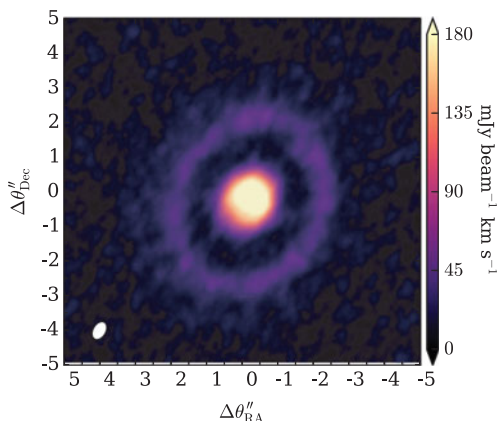


**Figure 7.**  $C_2H$   $N = 3 - 2$  (integrated over all hyperfine components) as observed in the DM Tau protoplanetary disk. The center is saturated by the color scheme in order to enhance the visibility of the faint outer ring. Data from Bergin *et al.* (2016).

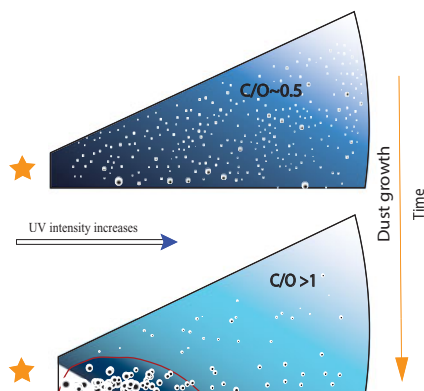


**Figure 8.** Evolution of the  $C/O$  ratio with time by dust growth, settling, and dust radial drift. Oxygen is preferentially sequestered as water ice on cold grains. Figure credit Ke Zhang.

The same work also imaged the DM Tau  $C_2H$  distribution, which was found to occupy not one but two separate rings (see Figure 7). The inner ring appears just outside of the brightest peak of dust emission, suggesting possible dust extinction effects impacting the observable line emission, i.e., a “false” hole. The second ring, however, nests outside of DM Tau’s disk of millimeter emission. Thus there appears to be some relationship between the hydrocarbon emission and a lack of large grains.

Additional chemical modeling of  $C_2H$  found that the brightness of line required large column densities ( $\gtrsim 10^{14} \text{ cm}^{-2}$ ). To reach the necessary abundances required a severe depletion of oxygen (i.e.,  $C/O \gg 1$ ; Bergin *et al.* 2016). Correspondingly, the brightness of  $C_2H$  naturally fits with the picture of a lack of oxygen (water) relative to carbon as described in Section 3. Thus the relationship with the dust grain edge may suggest that the water/oxygen mass has been sequestered into the larger grains closer to the star, leaving a region of high  $C/O$  in the outer disk and upper layers (see Figure 8).

### 3.3. Organics

The sensitivity improvements of ALMA also enabled the first detection of organics in a protoplanetary disk. Perhaps more surprising, however, was that the first organics found

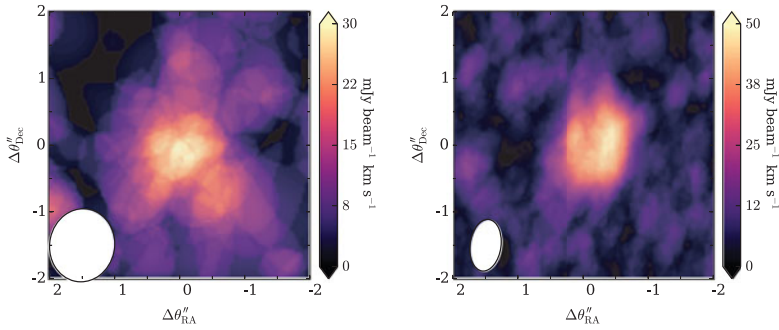


**Figure 9.** Methyl cyanide (left) and cyanoacetylene (right) observed toward the MWC 480 disk with ALMA. Data are from Öberg *et al.* (2015b).

were not the “usual suspects” as were expected from observations of protostars, e.g., methanol (e.g., Herbst & van Dishoeck 2009, and references therein). Instead, the first complex species observed in disks were methyl cyanide ( $\text{CH}_3\text{CN}$ ) and cyanoacetylene ( $\text{HC}_3\text{N}$ ) as reported in Öberg *et al.* (2015b), see Figure 9.

Shortly thereafter, methanol was detected in the TW Hya disk (Walsh *et al.* 2016), but its abundance was strongly over-predicted by models. As methanol forms by hydrogen addition to CO ice, it may be that the sequestration of carbon and/or oxygen from CO starves off the local production of observable methanol. This does not imply that disks are globally methanol poor, but rather the upper layers where methanol comes off the grain show a deficit, similar to water.

## 4. Disk Energetic Processes and Consequences

### 4.1. Disk ionization

Ionization plays an important role in both the physical properties and the volatile composition of protoplanetary disks. High energy photons/particles with energies exceeding  $E > 13.6$  eV are able to act on the bulk  $\text{H}_2$  and helium gas, impacting e.g., disk heating and coupling efficiency to the magnetic fields. Chemically, ionization impacts both gas and grain abundances in disks (Cleeves *et al.* 2014; Eistrup *et al.* 2016). At low temperatures ( $\lesssim 100$  K) gas-phase chemistry proceeds through ion-neutral reactions. Simultaneously, much of the rich interstellar grain-surface chemistry requires a source of atomic hydrogen, where ionization of  $\text{H}_2$  is a key production term.

The key sources of high energy ionization include X-rays, cosmic rays, and short-lived radionuclides. X-rays from the central star are obstructed by the inner disk except for those at very high energies ( $> 5$  keV). Cosmic rays are thought to be the most important ionization source for the X-ray-shielded outer disk; however, in the presence of stellar/disk winds or magnetic fields, CRs are easily deflected (Turner & Drake 2009; Cleeves *et al.* 2013). Radionuclides have uncertain abundances depending on the local history of star formation, especially massive stars, and how these materials are delivered to the disk (e.g., Adams 2010).

In Cleeves *et al.* (2014), we identified that observations of  $\text{HCO}^+$ ,  $\text{H}^{13}\text{CO}^+$  and  $\text{N}_2\text{H}^+$  can be used in concert to measure the ionization rate and its sources, in particular X-rays versus cosmic rays. We applied these techniques to observations of the well-constrained TW Hya disk with the SMA and ALMA to measure its disk-averaged ionization rate (Cleeves *et al.* 2015). We found low CR models (a factor of  $\gtrsim 100$  reduction) systemati-

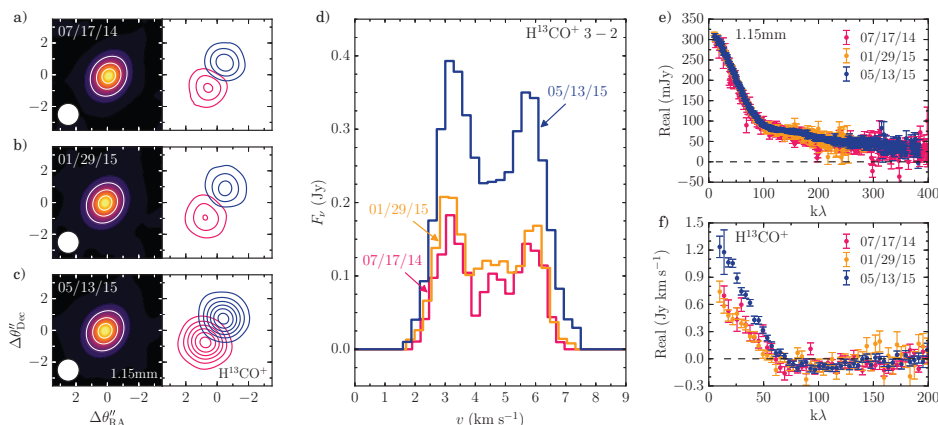


**Figure 10.**  $\text{H}^{13}\text{CO}^+$   $J = 3 - 2$  toward the IM Lup protoplanetary disk as measured at three different epochs with ALMA. The velocity integrated line flux doubles relative to a constant continuum flux, which is visible in the image (left), spectral (middle), and visibility (right) domains. Figure taken with permission from Cleeves *et al.* (2017).

cally fit the data better. Thus the outer disk was far more ionization poor than expected by conventional physical models.

#### 4.2. Time dependent ionization chemistry?

To extend upon our study of TW Hya, we obtained spatially resolved data to study the ionization properties of the IM Lup protoplanetary disk. However, upon inspection we discovered that the flux of one of the key molecular ions,  $\text{H}^{13}\text{CO}^+$ , was not constant in time over the year the ALMA observations were carried out (see Figure 10). Initial models presented in Cleeves *et al.* (2017) show that variability in the incident X-ray flux (as expected from X-ray flares from young stars), can cause short-term chemical changes in the atmospheric abundances of the disk. The impact on  $\text{H}^{13}\text{CO}^+$  is lessened in the shielded parts of the disk where densities are high (quenching the enhancement in the ionization fraction) and the X-ray fluxes are low.

While these short-term events may not impact the bulk chemistry in the densest parts of the disk, time-domain observations of molecular ions in disk may provide new insights into the ionization fraction in the upper layers of the disk where the disappearance time of the effect is directly related to the local electron density.

#### 4.3. Gas kinematics and turbulence

The low global ionization rates, and particularly the lack of evidence for cosmic ray ionization in the outer disk from Cleeves *et al.* (2015), is expected to reduce the efficiency of coupling between the gas and disk magnetic fields. Such coupling is necessary for the magnetorotational instability (MRI; Balbus & Hawley 1991) to operate as a source of viscosity for disk accretion.

MRI is expected to generate additional non-thermal motions that should be detectable with high spectral resolution observations (Simon *et al.* 2015). Flaherty *et al.* (2015) carried out parameterized modeling to isolate non-thermal motions in the HD163296 disk. They find an upper limit for line broadening due to turbulence of  $< 3\%$  of the local sound speed. These limits are an order of magnitude lower than theory would predict, suggesting that MRI is less efficient beyond 30 AU than previously considered. Recent work on the 3D structure of turbulence by Flaherty *et al.* (2017) support this picture, and add that turbulence is low throughout the vertical extent of the disk. Note

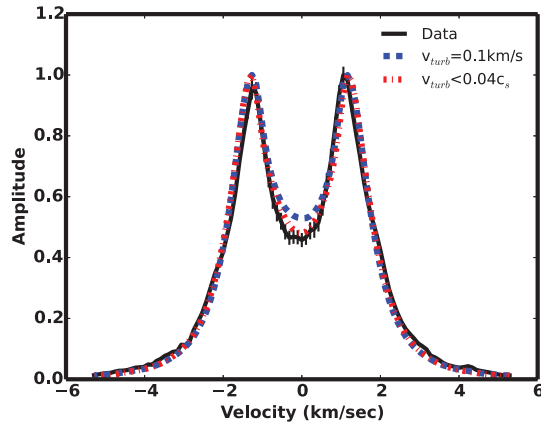


**Figure 11.** Normalized disk integrated spectra of CO  $J = 3-2$  toward HD163296. The data are fit better by models with little to no turbulence (red dashed line) than with turbulence typical of MRI (blue dashed line). Reproduced with permission from Flaherty *et al.* (2015).

additional measurements by Teague *et al.* (2016) who use optically thick lines to constrain temperature find a larger value for turbulent broadening; however, they state that even these should be considered upper limits given the systematics in the data.

## 5. An emerging understanding and implications

As each result comes out, we can begin to assemble a broader picture of the protoplanetary disk physical and chemical environment over the first few Myr. Early observations of depleted oxygen and carbon from the SMA, ALMA, and *Herschel* pointed to rapid sequestration of volatiles potentially in the form of ices on larger grains. These findings imply that vertical mixing cannot be very efficient at dredging up material in the outer disk (beyond 10 AU), otherwise the upper layers would be replenished in their observable volatile content. This picture is consistent with measured low ionization rates in TW Hya, which can reduce the efficiency of MRI driven turbulence, likewise explaining the strong upper limits to non-thermal motions observed.

As such, a consistent picture is emerging between the physical nature of the disk and its chemical content. A less vigorously mixed disk tends to be less chemically altered, which may act to preserve more of the initial composition of the disk at formation. However it should be emphasized that the results described in this contribution come from disks spanning a wide variety of ages, physical environments, and stellar masses. This “emerging picture” is only just the beginning and will undoubtedly be continuously revised with new data. Furthermore, we are still at a phase where we do not yet fully understand the “massive” disks toward which we are observationally biased. Future chemical surveys in the coming years, especially those targeting lower mass disks, will hopefully tell us whether the intuition we are building towards the massive end holds in general for planet formation across the disk/stellar mass spectrum.

## References

- Adams, F. C. 2010, *ARA&A*, 48, 47  
 Aikawa, Y., Furuya, K., Nomura, H., & Qi, C. 2015, *ApJ*, 807, 120  
 ALMA Partnership, Brogan, C. L., Pérez, L. M., Hunter, T. R., *et al.* 2015, *ApJL*, 808, L3  
 Andrews, S. M., Wilner, D. J., Hughes, A. M., *et al.* 2012, *ApJ*, 744, 162

- Andrews, S. M., Wilner, D. J., Zhu, Z., Birnstiel, T., Carpenter, J. M., Pérez, L. M., Bai, X.-N., Öberg, K. I., Hughes, A. M., Isella, A., & Ricci, L. 2016, *ApJL*, 820, L40
- Balbus, S. A. & Hawley, J. F. 1991, *ApJ*, 376, 214
- Bergin, E. A., Aikawa, Y., Blake, G. A., & van Dishoeck, E. F. 2007, *Protostars and Planets V*, 751
- Bergin, E. A., Alves, J., Huard, T., & Lada, C. J. 2002, *ApJL*, 570, L101
- Bergin, E. A., Cleeves, L. I., Gorti, U., Zhang, K., Blake, G. A., Green, J. D., Andrews, S. M., Evans, II, N. J., Henning, T., Öberg, K., Pontoppidan, K., Qi, C., Salyk, C., & van Dishoeck, E. F. 2013, *Nature*, 493, 644
- Bergin, E. A., Du, F., Cleeves, L. I., Blake, G. A., Schwarz, K., Visser, R., & Zhang, K. 2016, *ApJ*, 831, 101
- Bergin, E. A., Hogerheijde, M. R., Brinch, C., Fogel, J., Yıldız, U. A., Kristensen, L. E., van Dishoeck, E. F., Bell, T. A. *et al.* 2010, *A&A*, 521, L33
- Charnley, S. B. 1997, *MNRAS*, 291, 455
- Cleeves, L. I. 2015, *PhD thesis*, University of Michigan
- . 2016, *ApJL*, 816, L21
- Cleeves, L. I., Adams, F. C., & Bergin, E. A. 2013, *ApJ*, 772, 5
- Cleeves, L. I., Bergin, E. A., & Adams, F. C. 2014, *ApJ*, 794, 123
- Cleeves, L. I., Bergin, E. A., Öberg, K. I., Andrews, S., Wilner, D., & Loomis, R. 2017, *ApJL*, 843, L3
- Cleeves, L. I., Bergin, E. A., Qi, C., Adams, F. C., & Öberg, K. I. 2015, *ApJ*, 799, 204
- Du, F., Bergin, E. A., Hogerheijde, M., van Dishoeck, E. F., Blake, G., Bruderer, S., Cleeves, L., Dominik, C., Fedele, D., Lis, D. C., Melnick, G., Neufeld, D., Pearson, J., & Yıldız, U. 2017, *ApJ*, 842, 98
- Eistrup, C., Walsh, C., & van Dishoeck, E. F. 2016, *A&A*, 595, A83
- Favre, C., Cleeves, L. I., Bergin, E. A., Qi, C., & Blake, G. A. 2013, *ApJL*, 776, L38
- Flaherty, K. M., Hughes, A. M., Rose, S. C., Simon, J. B., Qi, C., Andrews, S. M., Kóspál, Á., Wilner, D. J., Chiang, E., Armitage, P. J., & Bai, X.-n. 2017, *ApJ*, 843, 150
- Flaherty, K. M., Hughes, A. M., Rosenfeld, K. A., Andrews, S. M., Chiang, E., Simon, J. B., Kerzner, S., & Wilner, D. J. 2015, *ApJ*, 813, 99
- Glassgold, A. E., Najita, J., & Igea, J. 1997, *ApJ*, 480, 344
- Guzmán, V. V., Öberg, K. I., Huang, J., Loomis, R., & Qi, C. 2017, *ApJ*, 836, 30
- Guzmán, V. V., Öberg, K. I., Loomis, R., & Qi, C. 2015, *ApJ*, 814, 53
- Herbst, E. & van Dishoeck, E. F. 2009, *ARA&A*, 47, 427
- Hily-Blant, P., Magalhaes, V., Kastner, J., Faure, A., Forveille, T., & Qi, C. 2017, *A&A*, 603, L6
- Hogerheijde, M. R., Bekkers, D., Pinilla, P., Salinas, V. N., Kama, M., Andrews, S. M., Qi, C., & Wilner, D. J. 2016, *A&A*, 586, A99
- Hogerheijde, M. R., Bergin, E. A., Brinch, C., *et al.* 2011, *Science*, 334, 338
- Huang, J., Öberg, K. I., & Andrews, S. M. 2016, *ApJL*, 823, L18
- Huang, J., Öberg, K. I., Qi, C., Aikawa, Y., Andrews, S. M., Furuya, K., Guzmán, V. V., Loomis, R. A., van Dishoeck, E. F., & Wilner, D. J. 2017, *ApJ*, 835, 231
- Isella, A., Guidi, G., Testi, L., Liu, S., Li, H., Li, S., Weaver, E., Boehler, Y., Carpenter, J. M., De Gregorio-Monsalvo, I., Manara, C. F., Natta, A., Pérez, L. M., Ricci, L., Sargent, A., Tazzari, M., & Turner, N. 2016, *Physical Review Letters*, 117, 251101
- Kama, M., Bruderer, S., Carney, M., *et al.* 2016, *A&A*, 588, A108
- Kamp, I., Thi, W.-F., Meeus, G., Woitke, P., Pinte, C., Meijerink, R., Spaans, M., Pascucci, I., Aresu, G., & Dent, W. R. F. 2013, *A&A*, 559, A24
- Kastner, J. H., Qi, C., Gorti, U., Hily-Blant, P., Öberg, K., Forveille, T., Andrews, S., & Wilner, D. 2015, *ApJ*, 806, 75
- McClure, M. K., Bergin, E. A., Cleeves, L. I., van Dishoeck, E. F., Blake, G. A., Evans, II, N. J., Green, J. D., Henning, T., Öberg, K. I., Pontoppidan, K. M., & Salyk, C. 2016, *ApJ*, 831, 167
- Millar, T. J. 2003, *Space Sci. Rev.*, 106, 73

- Nomura, H., Tsukagoshi, T., Kawabe, R., Ishimoto, D., Okuzumi, S., Muto, T., Kanagawa, K. D., Ida, S., Walsh, C., Millar, T. J., & Bai, X.-N. 2016, *ApJL*, 819, L7
- Öberg, K. I., Furuya, K., Loomis, R., Aikawa, Y., Andrews, S. M., Qi, C., van Dishoeck, E. F., & Wilner, D. J. 2015a, *ApJ*, 810, 112
- Öberg, K. I., Guzmán, V. V., Furuya, K., Qi, C., Aikawa, Y., Andrews, S. M., Loomis, R., & Wilner, D. J. 2015b, *Nature*, 520, 198
- Qi, C., Öberg, K. I., Andrews, S. M., Wilner, D. J., Bergin, E. A., Hughes, A. M., Hogherheijde, M., & D'Alessio, P. 2015, *ApJ*, 813, 128
- Qi, C., Öberg, K. I., Wilner, D. J., D'Alessio, P., Bergin, E., Andrews, S. M., Blake, G. A., Hogherheijde, M. R., & van Dishoeck, E. F. 2013, *Science*, 341, 630
- Salinas, V. N., Hogherheijde, M. R., Mathews, G. S., Öberg, K. I., Qi, C., Williams, J. P., & Wilner, D. J. 2017, ArXiv e-prints
- Schwarz, K. R., Bergin, E. A., Cleeves, L. I., Blake, G. A., Zhang, K., Öberg, K. I., van Dishoeck, E. F., & Qi, C. 2016, *ApJ*, 823, 91
- Simon, J. B., Hughes, A. M., Flaherty, K. M., Bai, X.-N., & Armitage, P. J. 2015, *ApJ*, 808, 180
- Teague, R., Guilloteau, S., Semenov, D., Henning, T., Dutrey, A., Piétu, V., Birnstiel, T., Chapillon, E., Hollenbach, D., & Gorti, U. 2016, *A&A*, 592, A49
- Teague, R., Semenov, D., Gorti, U., Guilloteau, S., Henning, T., Birnstiel, T., Dutrey, A., van Boekel, R., & Chapillon, E. 2017, *ApJ*, 835, 228
- Testi, L., Birnstiel, T., Ricci, L., Andrews, S., Blum, J., Carpenter, J., Dominik, C., Isella, A., Natta, A., Williams, J. P., & Wilner, D. J. 2014, *Protostars and Planets VI*, 339
- Thi, W.-F., Mathews, G., Ménard, *et al.* 2010, *A&A*, 518, L125
- Trilling, D. E., Koerner, D. W., Barnes, J. W., Ftaclas, C., & Brown, R. H. 2001, *ApJL*, 552, L151
- Turner, N. J. & Drake, J. F. 2009, *ApJ*, 703, 2152
- van der Marel, N., van Dishoeck, E. F., Bruderer, S., *et al.* 2013, *Science*, 340, 1199
- van't Hoff, M. L. R., Walsh, C., Kama, M., Facchini, S., & van Dishoeck, E. F. 2017, *A&A*, 599, A101
- Walsh, C., Loomis, R. A., Öberg, K. I., Kama, M., van 't Hoff, M. L. R., Millar, T. J., Aikawa, Y., Herbst, E., Widicus Weaver, S. L., & Nomura, H. 2016, *ApJL*, 823, L10
- Zhang, K., Bergin, E. A., Blake, G. A., Cleeves, L. I., & Schwarz, K. R. 2017, *Nature Astronomy*, 1, 0130